Structural Studies of the Hemocyanin Active Site. 2. Resonance Raman Spectroscopy

James A. Larrabee and Thomas G. Spiro*

Contribution from the Department of Chemistry, Princeton University, Princeton, New Jersey 08540. *Received November 26, 1979*

Abstract: Raman spectra of oxyhemocyanin, excited in resonance with the intense 345-nm absorption, show strong enhancement of modes below 350 cm^{-1}, some of which are assignable to copper–imidazole stretching vibrations via $^{63}Cu/^{65}Cu$ and H_2O/D_2O frequency shifts. Arthropod and mollusc proteins show somewhat different intensity patterns, although different species within the same class show the same pattern. The isotope shifts imply an asymmetric disposition of the imidazole ligands, and the frequencies are consistent with two imidazoles sharing a tetragonal plane with the ligands bridging the two Cu^{2+} ions, and a third imidazole occupying an apical position. Enhancement of the O–O stretching mode is much lower, and is comparable to that observed for resonance with the 570-nm absorption band, despite the 20-fold lower absorptivity of the latter. The implied disparity in the Franck–Condon products associated with the two transitions is consistent with their assignment to charge-transfer transitions from the two different O_2^{2-} π^* orbitals. The higher energy transition is associated with the lower energy orbital, which is less antibonding with respect to the O–O bond. Surprisingly, the $Cu-O_2$ stretching mode has not been detected; its intensity must be at least fivefold lower than that of the O–O stretch. A broad (~50 cm^{-1}) Raman band is seen at 1075 cm^{-1}, which is attributable to an electronic Raman effect. Assignment to the singlet → triplet transition of the coupled Cu^{2+} pair is suggested.

Introduction

In the preceding article[1] a model for the hemocyanin (Hc) oxygen binding site was proposed, based on extended X-ray absorption fine structure (EXAFS) measurements and on near-ultraviolet (UV) resonance Raman (RR) spectroscopy. The RR results are the subject of the present paper. Previous RR studies by Loehr and co-workers[2-4] using laser excitation within the oxyhemocyanin visible absorption band produced valuable insights into the nature of oxygen binding. The identification of the O–O stretch near 750 cm^{-1} via $^{18}O_2$ substitution established that the electronic structure of the bound dioxygen is essentially that of peroxide, and strengthened the inference that the copper atoms are Cu^{2+} arranged in antiferromagnetically coupled pairs.[5] Use of the isotopically mixed molecule $^{16}O-^{18}O$ established that the two ends of the bound dioxygen molecule are essentially equivalent,[4] in contrast to the situation found for hemerythrin[6] for which a distinct inequivalence is observed. Excitation profiles[3] showed that the O–O stretching mode was enhanced via two closely spaced visible transitions, both assignable to $O_2^{2-} \rightarrow Cu^{2+}$ charge-transfer transitions, while a low frequency mode, near 270 cm^{-1}, showed preresonance enhancement via the intense near-UV band at 345 nm. Direct excitation into this band[7] has revealed a rich assortment of RR bands between 100 and 350 cm^{-1}, which were ascribed to vibrational modes of the copper coordination group. In the present work we have been able to identify the most intense of these features with copper–imidazole stretching modes in an asymmetric complex, using $^{63}Cu/^{65}Cu$ and H_2O/D_2O frequency shifts. In addition we have observed a broad band, at ~1075 cm^{-1}, assignable to an electronic Raman mode, resonant with the 345-nm absorption band. It is tentatively ascribed to the singlet–triplet transition of the coupled Cu_2^{2+} unit.

Experimental Section

Protein Preparations. Live *Busycon canaliculatum* specimens (channeled whelks, mollusc) were obtained from Marine Biological Laboratories, Woods Hole, Mass. A small opening was made in the shell, the cardiac chamber was exposed, the heart punctured, and the hemolymph was removed by syringe and transferred to cold centrifuge tubes. The blood was centrifuged at low speed to remove debris and was exhaustively dialyzed against distilled water or buffer at 4 °C. Hc accounts for over 95% of the total protein prepared in this manner, and its concentration was estimated by absorption at 345 nm (ϵ = 10 000 M_{Cu}^{-1} cm^{-1}). The natural concentration of Hc (~1 mM in Cu) is ideal for RR studies in the intense 345-nm absorption band; for experiments in the visible region, the protein was concentrated (up to 7 mM in Cu) by ultrafiltration or centrifugation at 45000*g* for 6 h, and redissolution of the pellet in the buffer. A 0.05 M sodium carbonate buffer, pH 9.8, was used to minimize protein aggregation[9] which leads to turbid solutions at lower pH. *Megathura crenulata* (keyhole limpet, mollusc) Hc was obtained as an ammonium sulfate slurry from Pacific Biomarine Supply Co. (Venice, Calif.). The slurry was dialyzed against 0.01 M sodium phosphate buffer, pH 7.0, containing 1 M sodium chloride, any precipitate formed was removed by centrifugation at 10000*g*, and the supernatant was dialyzed against sodium carbonate buffer and concentrated. *Limulus polyphemus* (horseshoe crab, arthropod) blood was obtained from Marine Biological Laboratories. The hemolymph was centrifuged at low speed to remove cells and other debris; the protein solution was dialyzed against sodium carbonate buffer and concentrated (ϵ_{340} = 8500 M_{Cu}^{-1} cm^{-1}). *Cancer magister* (Pacific crab, arthropod) Hc was provided by Professor H. S. Mason of the University of Oregon, and *C. borealis* and *C. irroratus* (arthropods) Hc were supplied by Professor E. I. Solomon of the Massachusetts Institute of Technology.

For bound $^{18}O_2$ experiments, oxyHc was deoxygenated by passing water-saturated argon over a stirred solution for 24 h and reoxygenated with $^{18}O_2$ (Stohler Chemicals, >99% isotopic purity). D_2O solution were prepared by dialysis against D_2O buffer in an ultrafiltration cell. Copper isotope substitution was carried out with apoHc (*B. canaliculatum*), prepared by exhaustive dialysis (four changes) of hemocyanin (2 mM) against 20 volumes of 10 mM KCN in 26 mM sodium borate buffer, pH 8.5. Most of the cyanide was then removed by dialysis, and the last traces were removed by passing the apoprotein through a column of Sephadex G-25, equilibrated with the sodium borate buffer. Copper removal was estimated to be 95%, by comparison of A_{280}/A_{345} with oxyHc. Reconstitution[10] was carried out by incubation with isotopically pure Cu_2O prepared[11] by reducing CuO (^{63}Cu, 99.89%, or ^{65}Cu, 99.70%, obtained from Oak Ridge National Laboratories). Cu_2O (25 mg) (40-fold excess) was added to 20 mL of deoxygenated 0.7 mM apoHc, and the slurry was stirred under water-saturated N_2 for 5 days at 4 °C. The slurry was centrifuged at 15000*g* for 30 min, and the clear protein solution was passed through Chelex 100 resin to remove any adventitiously bound metal; 60–75% reconstitution was achieved, as determined by A_{280}/A_{345}. This procedure is particularly useful for working with isotopes since the unreacted cuprous oxide can be washed and reused.

The model complexes $Cu(1mH)_4Cl_2$, $Cu(1\text{-}MeIm)_4Cl_2$, $Cu(2\text{-}MeImH)_4Cl_2$, and $Cu(2\text{-}MeIm)_2$ (1mH, imidazole; MeImH, methylimidazole) were prepared according to Eilbeck et al.[12]

Raman spectra were excited with the 333.6-, 335.1-, and 351.1-, and 363.8-nm as well as the visible lines of a Spectra Physics 170 argon laser, and recorded with a Spex 1401 double monochromator with RCA C31034A photomultiplier and photon counting electronics.

0002-7863/80/1502-4217$01.00/0

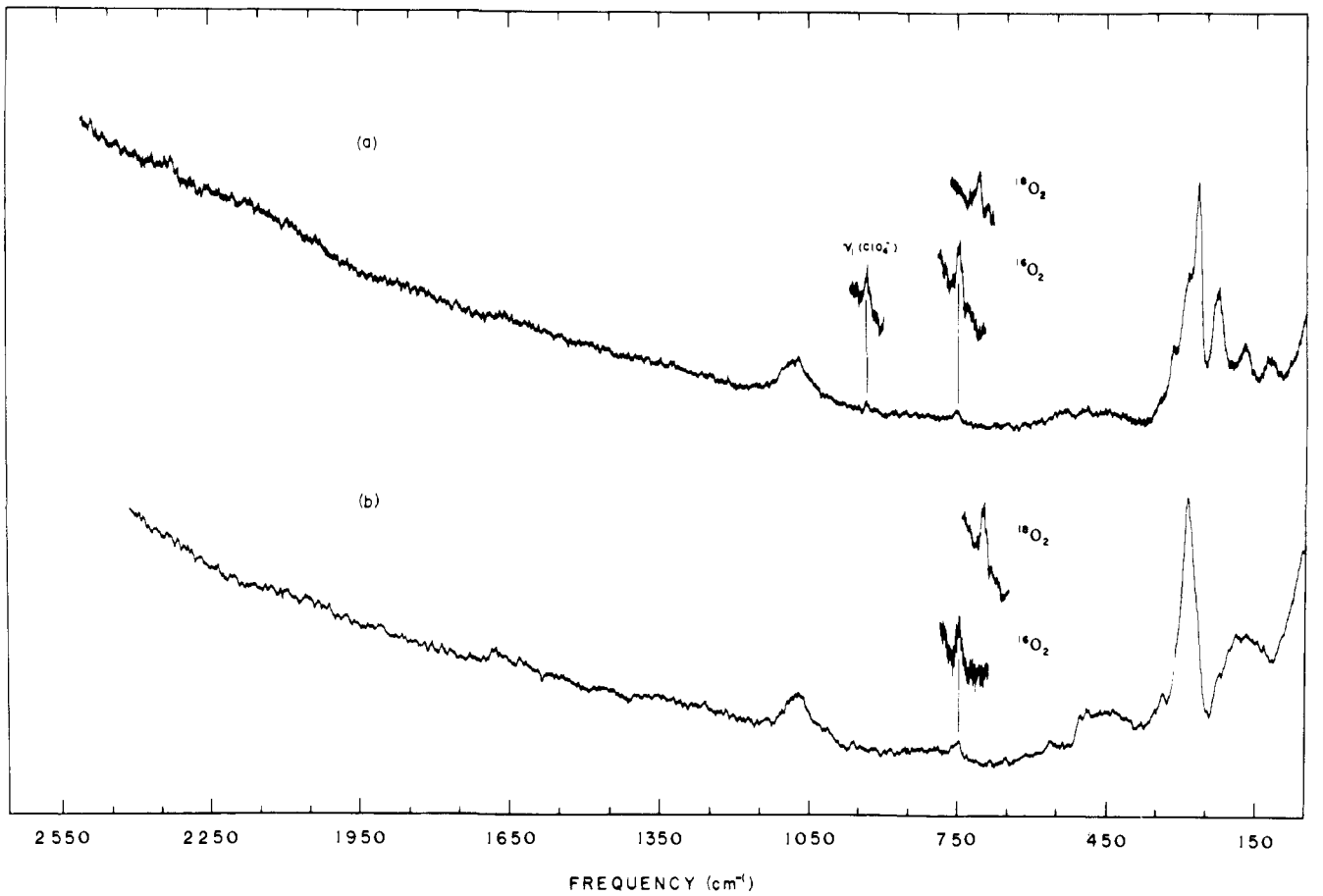

Figure 1. Raman spectra with 363.8-nm laser excitation (100 mW) of (a) 1 mM *B. canaliculatum* and (b) 1.4 mM *L. polyphemus* oxyhemocyanin, in 0.05 M sodium carbonate buffer, pH 9.8. In (a) 0.2 M $NaClO_4$ was present as an internal standard. Spectrometer conditions: spectral slit width, 7 (a) and 12 (b) cm^{-1}; sensitivity, 2000 (a and b) and 400 (inset peaks) Hz; rise time, 3 (a and b) and 10 (insets) s; scan speed, 30 (a), 60 (b), and 6 (insets) cm^{-1}/min.

Table I. Comparison of Resonance Raman Spectra of Oxyhemocyanins (cm^{-1})

B. canaliculatum	*M. crenulata*	*L. polyphemus*	*C. magister*	*C. irroratus*	*C. boreolis*
119	114				
170	173	180 br	180 br	110–240 br	199 br
226	228	223	218		217
267	267	271 sh	262 sh		
286 sh[a]	285 sh	287	282	288	284
315 sh	307 sh	306 sh	308 sh		
337 sh	337 sh	338	333 sh		332
749	746	752	744		748

[a] sh = shoulder; br = broad.

Spectra for calculating difference spectra ($^{16}O_2$-$^{18}O_2$ vide infra) were digitally recorded using an Ortec photon counter and Data General Nove 3 computer. Protein solutions were run in a spinning cell, which was modified for gas exchange in the $^{18}O_2$ experiments. Concentrated protein samples were run in a flow capillary system[13] or in backscattering.[14] Spectra were obtained shortly after protein preparation, since prolonged storage (1 week) led to significant increases in the background. The model compounds were run as solutions in a spinning cell, or in a spinning pellet holder as powdered solids pressed into KBr pellets.

Results

General Spectral Features. Figure 1 shows full Raman spectral scans for *Busycon* and *Lumulus* oxyHc, with 363.8-nm laser excitation. Strong scattering is observed, with multiple peaks, below 350 cm^{-1}. The O-O stretching mode, identifiable by the $^{18}O_2$ frequency shift, is observable as a weak peak near 750 cm^{-1}. A broad (~50 cm^{-1} full width at half-height) band can be seen at ~1075 cm^{-1}. Otherwise, the spectra are featureless, save for the slowly rising fluorescence background. Appreciable differences in detail can be seen between the two proteins, reflecting altered relative intensities and peak resolution, as reported previously.[7] These differences are characteristic for arthropods and molluscs. Table I lists band frequencies for the two mollusc and four arthropod hemocyanins surveyed in the present study.

Low-Frequency Isotope Shifts and Assignments. Figure 2 shows RR spectra, taken at high resolution in the low-frequency region, for isotopically reconstituted *Busycon* Hc. The isotopic purity of these samples is estimated to be 97% for ^{63}Cu and 94% for ^{65}Cu from the CuO isotopic purity and the extent of copper removal (95%) and reconstitution (60%) of the Hc. Distinct shifts are observed of 1.8, 2.3, and 2.8 cm^{-1} for the bands at 287, 267, and 227 cm^{-1}, respectively. These shifts are comparable to those found in the infrared spectra of copper complexes.[15] Thus, the $Cu(ImH)_4Cl_2$ IR band at 286 cm^{-1} shifts 3 cm^{-1} on $^{63}Cu/^{65}Cu$ substitution. The Raman bands

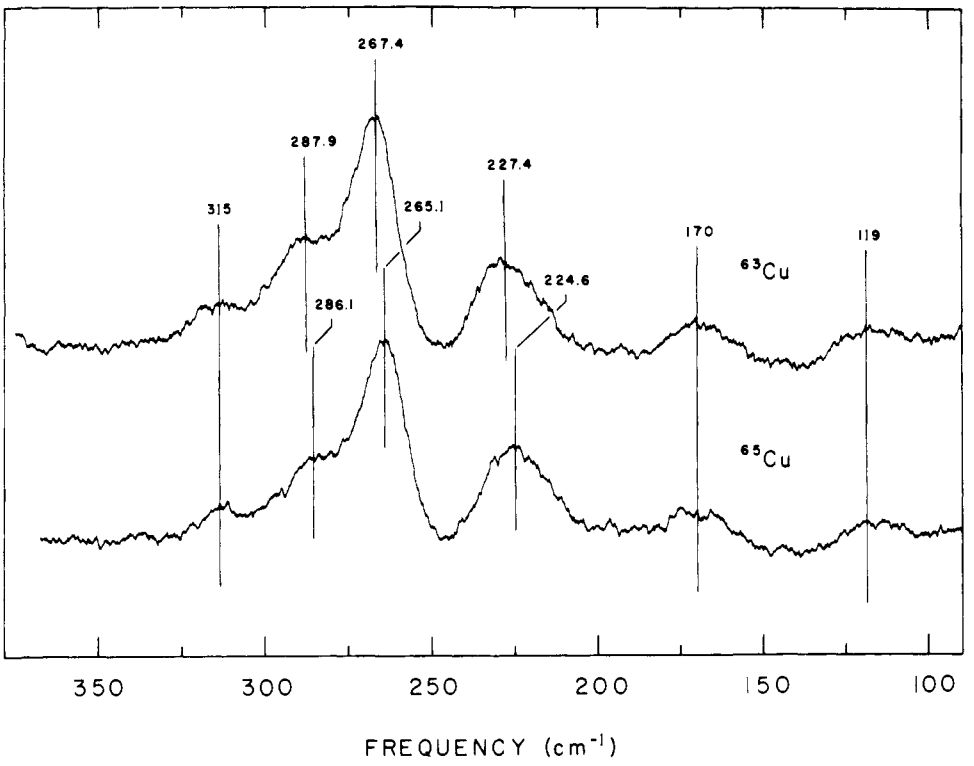

Figure 2. Raman spectra with 363.8-nm excitation (100 mW) of ^{63}Cu and ^{65}Cu. *B. canaliculatum* oxyhemocyanin (50 mg/mL) in 26 mM sodium borate buffer, pH 8.5. Conditions: spectral slit width, 6 cm^{-1}; sensitivity, 1000 Hz; rise time, 15 s; scan speed, 6 cm^{-1}/min.

are therefore conclusively associated with the copper coordination group. Moreover, the coordination group must be relatively asymmetric. If it approximated a regular tetrahedron, square, or triangle, then the breathing mode, which would be expected to be strongly Raman active, would involve no motion of the copper atom and therefore no isotope shift. The weak shoulders at 315 and 337 cm^{-1} (the latter is too weak to be recognizable in the high-resolution spectra) are insufficiently resolved to determine whether they are copper isotope sensitive. The bands at 170 and 119 cm^{-1}, although weak, are well enough resolved to determine that any isotope shift is less than 0.5 cm^{-1}. The lack of metal isotope sensitivity is consistent with their assignment to metal-ligand bending modes, which involve little motion of the metal atom.[15] Assignment to a symmetric breathing mode of the two copper ions in the active site (a "copper-copper stretch"), which is expected near 100 cm^{-1}, consistent with the EXAFS Debye-Waller factor,[1] is precluded.

Figure 3 compares *Busycon* Hc spectra at the same high resolution for a sample in H_2O with one in D_2O; 1.5- and 0.6-cm^{-1} shifts are observed for the 267 and 226 cm^{-1} bands, respectively. Although these shifts are small, they have been reproduced in several repeated scans. Shifts of this magnitude could not, however, have been detected in any of the other bands. Among the plausible protein ligands at the Hc active site, the only one with exchangeable protons is imidazole. The N1 proton exchanges immediately with solvent, while the C2 proton exchange is slow,[16] although it might be accelerated by coordination to copper. Table II lists Raman frequencies for $Cu(ImH)_4Cl_2$, a tetragonal Cu(II) complex with long axial Cu-Cl bonds, and the N1 and N1-C2 deuterated analogues. The frequencies above 800 cm^{-1} are associated with internal modes of the imidazole ligands; their frequencies and deuterium shifts are consistent with those previously observed for cobalt complexes.[17] The modes at 245 and 208 cm^{-1} are assignable to symmetric copper imidazole and copper chloride stretching, respectively.[12] The former shifts 1.2 cm^{-1} on N1 deuteration and 2.4 cm^{-1} on N1 and C2 deuteration. The D_2O shifts seen for the 267- and 226-cm^{-1} modes of oxyHc are therefore consistent with their assignment to copper imidazole stretching. Because of their lack of resolution, similar assignments cannot be ruled out for the 286-, 315-, and 337-cm^{-1} modes. One or two of them might alternatively be assigned to

Table II. Raman Frequencies of $Cu(ImH)_4Cl_2$ and Deuterated Derivatives (cm^{-1})

$Cu(ImH)_4Cl_2$	$Cu(ImH)_4Cl_2$ (N_1-D)	$Cu(ImH)_4Cl_2$ (N_1-D, C_2-D)	assignment[a]
1533	1514	1514	$\delta(R) + \delta(N_1\text{-}H)$
1490	1481	1466	$\delta(R) + \delta(C_2\text{-}H)$
1426 br	1355	1322	$\delta(N_1\text{-}H)$
	1423	1415	
		1397	
1408 sh			
1330	1322 br	1313	$\delta(R)$
1323 sh		1298 sh	
1256	1256	1205	$\delta(C_2\text{-}H)$
	1241		
	1169		
1168	1151 br	1145	$\delta(R) + \delta(N_1\text{-}H)$
1157			
1140	1121 sh	1121	$\delta(C_4,C_5\text{-}H) + \delta(R)$
1123	1113	1110 sh	
1106	1097	1092	$\delta(R) + \delta(C_4,C_5\text{-}H)$
1086	1084	1077	
1065	1063	959	$\delta(R) + \delta(C_2\text{-}H)$
	965		
	955		
946		938	$\delta(R)$
930		920	
913	903		$\omega(C_4,C_5\text{-}H)$
870	866	871	$\delta(R)$
		831	
245.0	243.8	242.6	$\nu(Cu\text{-}N)$
208.0	208.0	208.0	$\nu(Cu\text{-}Cl)$

[a] Based on ref 17; br = broad; sh = shoulder; $\delta(R)$ = ring deformation; ω = out-of-plane deformation; ν = stretch.

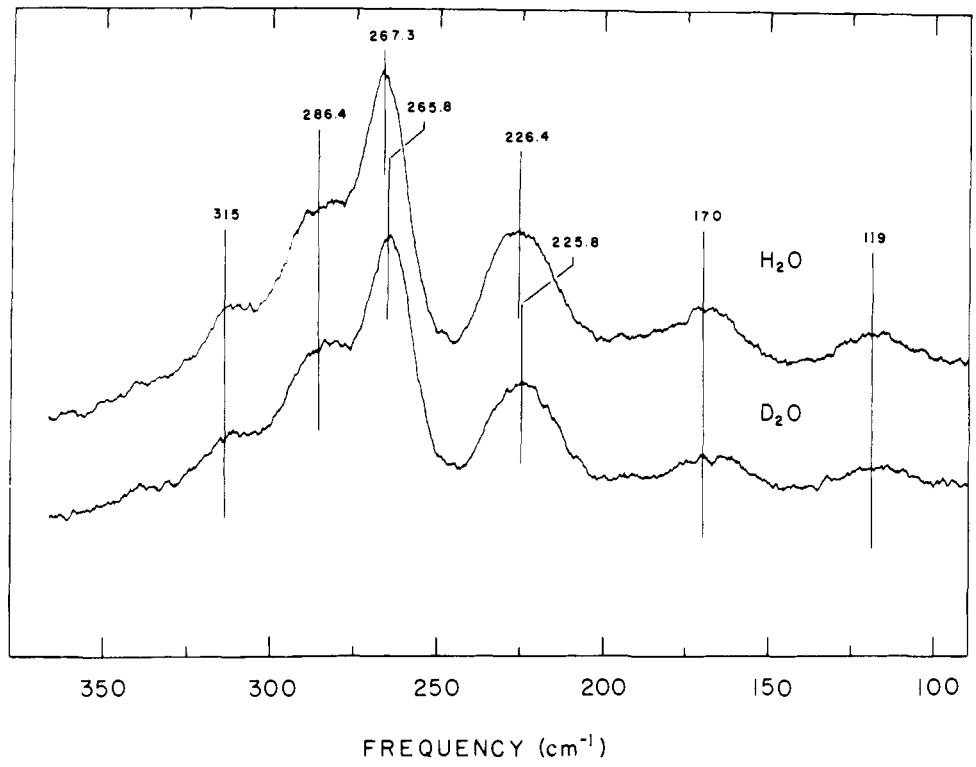

Figure 3. Raman spectra, as in Figure 4, of 1 mM *B. canaliculatum* oxyhemocyanin in H_2O and D_2O, 0.05 M sodium carbonate buffer, pH 9.8 and pD 9.4.

Table III. Copper Imidazole and Methylimidazole Stretching Frequencies

compd	ν_s, cm^{-1}	ν_{as}, cm^{-1}	ref
$Cu(ImH)_4Cl_2$	245	286	3, 15
$Cu(ImH)_4(NO_3)_2$	250	292	3, 15
$Cu(1\text{-}MeIm)_4Cl_2$	274		3
$Cu(2\text{-}MeImH)_4Cl_2$	276		3
$Cu(2\text{-}MeIm)_2$	248, 288	275	15
$Cu(1,2\text{-}diMeIm)_2Cl_2$	255	242, 261	3
$Cu(ImH)_2Cl_2$		307	15
$Cu(ImH)_2Br_2$		307	15

stretching modes of a bridging ligand, plausibly tyrosine,[1,18] which is believed to connect the copper ions, in addition to the bound O_2. If any of the observed modes were due to bound water or hydroxide, then a much larger frequency shift would have been observed in D_2O. Table III lists the frequencies of copper-imidazole stretching modes for copper complexes with imidazole and 1- and 2-methylimidazole, as observed in this study and in others.

O–O and Cu–O Stretching. Although weak in relation to the low-frequency bands, the O-O stretch is clearly observable in the oxyHc spectra, and the frequencies are listed in Table I. For *B. canaliculatum* and *C. magister*, they agree with those reported previously by Freedman et al.;[3] *M. crenulata* and *C. borealis* fall in the same range, while the *L. polyphemus* frequency is a little higher. The variability in the O-O frequency, though small, is outside of experimental error. There is, however, no correlation between arthropod and mollusc Hc, as is observed for the low-frequency modes.

We have searched carefully for the location of the $Cu-O_2$ stretching modes, with negative results. In hemerythrin the $Fe-O_2$ mode has been identified[19] by its $^{18}O_2$ shift, at 504 cm^{-1}. This region is featureless in our spectra (Figure 1), except for a contribution from glass scattering. We have subtracted an $^{18}O_2$ spectrum from an $^{16}O_2$ spectrum, and observed positive and negative peaks for the O-O stretch, but only noise everywhere else. If a Cu-O mode had been present with as much as 20% intensity of the O-O stretch, it would have been detected.

1075-cm^{-1} Electronic Band. Both arthropod and mollusc Hc show a broad moderate intensity band at 1075 cm^{-1} (see Figure 1). The bandwidth at half-height, ~50 cm^{-1}, is too large for a single vibrational mode. (ν_1 of CO_3^{2-}, present in the buffer, happens to fall at 1040 cm^{-1}, but it is much weaker and narrower than the Hc band, which was also observed in a sample prepared with borate buffer.) The band is definitely resonance enhanced via the 345-nm transition, following essentially the same excitation profile (see below) as the other Hc bands. Its frequency does not correspond to an overtone or combination level of the other resonance enhanced modes, nor to an internal mode of the imidazole ligands, nor to any other characteristic protein vibration; nonresonance protein spectra[20] show only weak scattering in this region, which is assigned[21] to C-N stretching vibrations. We conclude that this band arises from an electronic Raman transition based on copper.

Excitation Profiles. Figure 4 shows excitation profiles of the *Busycon* oxyHc Raman bands through the 345-nm absorption band, obtained with the near-UV argon laser lines. This includes the O-O stretching mode at 749 cm^{-1}, although its enhancement is only ~1/15 of the intense band at 267 cm^{-1}. The enhancement of the O-O mode in the 345-nm absorption band is essentially the same as it is in the 570-nm band, although the latter is only 1/20 as strong as the former.

Figure 5 contains excitation data for the complex $Cu(ImH)_4Cl_2$, which shows an absorption shoulder at ~330 nm, assignable to imidazole → copper charge transfer.[22] The internal imidazole modes at 1256 and 1330 cm^{-1} are seen to be enhanced in the near-UV, but the copper-imidazole and copper-chloride stretching modes at 245 and 208 cm^{-1}, respectively, are not enhanced.

Discussion

Absorption Bands. The intensity of the 345-nm electronic transition, ϵ = 10 000 M_{Cu}^{-1} cm^{-1}, indicates that it is electric dipole allowed. The dominant scattering mechanism is expected to be the *A* term,[23,24] which produces enhancement

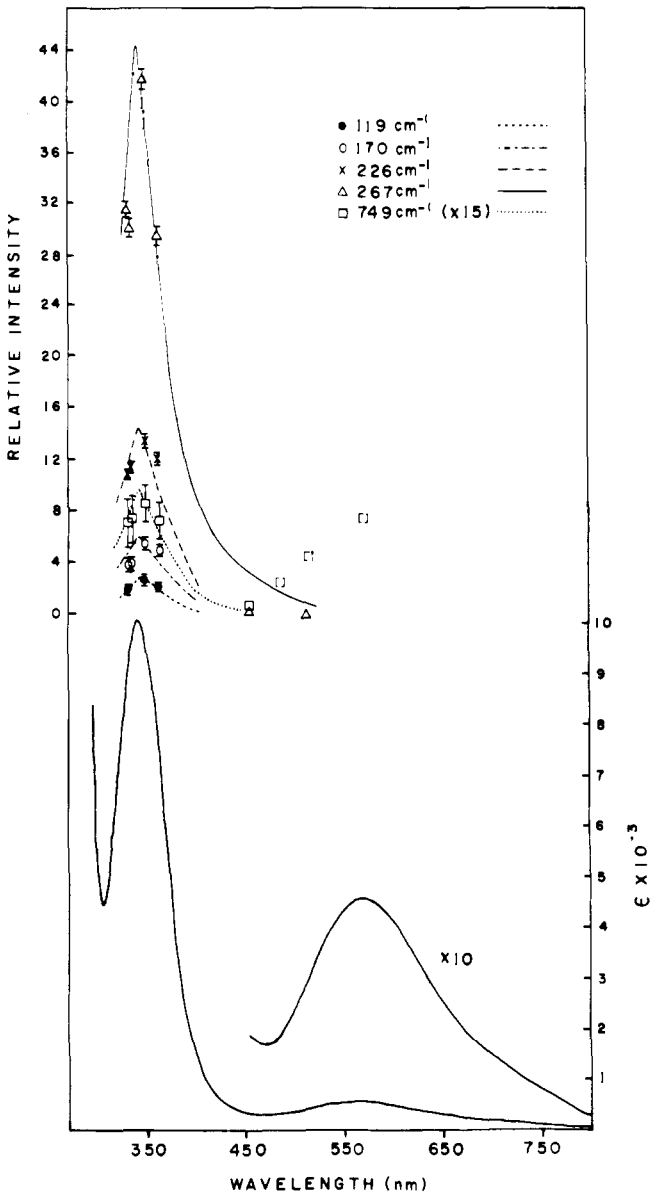

Figure 4. Raman excitation profiles for *B. canaliculatum* oxyhemocyanin, 1 mM for UV, 4.5 mM for visible wavelengths, in 0.05 M sodium carbonate buffer, pH 9.8. Intensities were measured relative to the ν_1 (935 cm^{-1}) band of 0.2 M $NaClO_4$ present as an internal standard. Error bars indicate the range of values for three separate measurements. The curves drawn through the data point represent the A term frequency dependence,[23,24] using the actual peak frequency (2.90 μm^{-1}) and half-bandwidth (0.2 μm^{-1}) of the 345-nm absorption band.

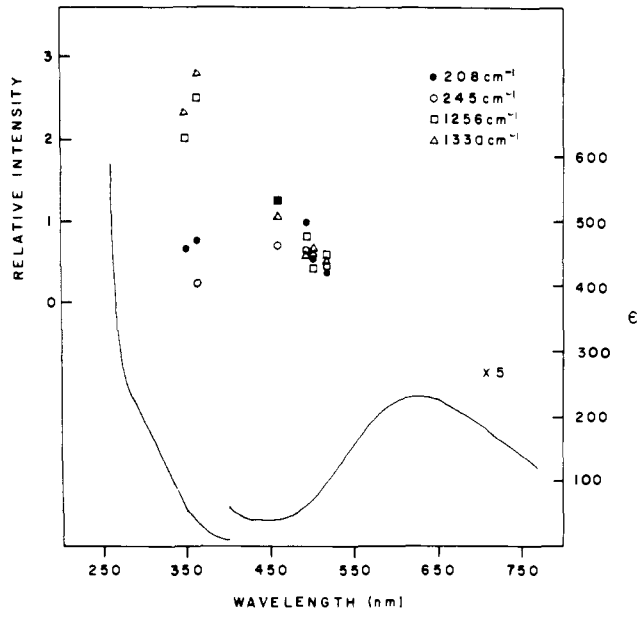

Figure 5. Absorption spectrum of $Cu(ImH)_4Cl_2$ (in H_2O) and relative Raman intensities for ν_{Cu-Cl} (208 cm^{-1}), ν_{Cu-Im} (245 cm^{-1}), and two internal imidazole modes (solid sample, mixed with Na_2SO_4 as an internal standard).

proportional to the square of the electronic transition moment and the Franck-Condon overlap product for the Raman mode. The relative intensities of the different vibrational modes are expected to reflect the extent to which they are involved in the geometric distortion in the excited state.[25]

The identity of this excited state is uncertain, and it has been the subject of debate. Assignment of the 345-nm transition of imidazole → copper charge transfer[3] seems unlikely in view of the absence of any detectable Raman intensity at the positions of the imidazole ring modes. Charge transfer from imidazole should weaken the internal imidazole bonds, leading to enhancement of the ring frequencies. Figure 7 shows that in a simple copper imidazole complex, the imidazole ring modes are indeed enhanced in the near-UV, in the vicinity of a band assignable to imidazole → copper charge transfer, whereas the copper-imidazole and copper-chloride stretching modes are not enhanced. The charge-transfer band is so weak, however, that the enhancement observed for the ring modes may actually be a preresonance effect from the much more intense imidazole transitions at higher energy. The high intensity and relatively low energy of the 345-nm hemocyanin transition also render an imidazole → copper charge-transfer assignment implausible.[22]

Assignment to a simultaneous pair excitation (SPE) involving a transition in which electrons on both Cu^{2+} ions are excited with a single photon[26] has been suggested as being consistent with the energy of the transition (roughly twice that of the Cu^{2+} d-d transitions) and with the observation that only copper-ligand vibrational modes appear to be strongly resonance enhanced.[7] The high intensity of the absorption renders this assignment problematic, however, as does the observation that in methemocyanin, an oxidized form of the protein in which the Cu^{2+} ions are also antiferromagnetically coupled, both the 570-nm visible band and the 345-nm near-UV bands are absent.[18] Solomon and co-workers[18] have suggested that both of these bands arise from peroxide → copper charge transfer, the transitions originating on different peroxide orbitals.

This assignment can be understood on the basis of the orbital diagram shown in Figure 6, which is a modification of the one given by Freedman et al.[3] The model for this diagram[1] is a complex of C_2 symmetry involving peroxide symmetrically bound to two Cu^{2+} ions. In this symmetry the two peroxide π^* orbitals are nonequivalent; one of them is symmetric (π^*_S) while the other is asymmetric (π^*_A) with respect to the C_2 axis. Each of the Cu^{2+} ions (d^9) has one half-filled d orbital, the others being filled. In Figure 6 the half-filled orbitals are shown as pointing in the direction of the peroxide oxygen atoms, in consonance with the substantial overlap implied by the charge-transfer intensities. Overlap with the copper orbitals will split the energies of the π^* orbitals, unless the dihedral angle about the oxygen-oxygen bond, β, happens to be 90°. The internuclear distances determined by EXAFS,[1] Cu-Cu = 3.67 Å and Cu-O = 1.96 Å, and the known bond distance for peroxide, 1.45 Å, do not fix the angle, γ, of the O-O bond with respect to the Cu-Cu vector, which could be anywhere from 0 to 90°. The corresponding ranges for the dihedral angle β and for the Cu-O-O angle α are 0 to 137° and 176 to 69°, respectively. For dihedral angles less than 90°, π^*_A is expected

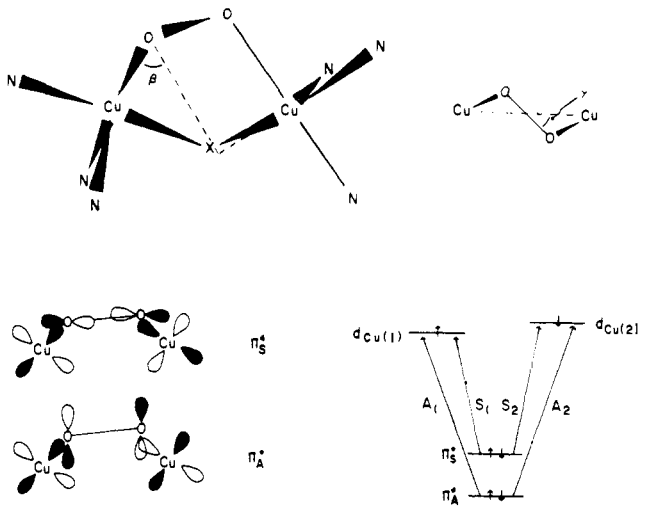

Figure 6. Model of the oxyHc binding site,[1] with orbital overlap and electronic transition diagrams.

to lie lower than π_S^*, because of more favorable overlap with the copper orbitals, as shown in Figure 6. Interactions with the filled Cu^{2+} orbitals will also influence the splitting, however.

The Cu^{2+} orbitals are coupled relatively weakly, as evidenced by the observation of d-d transitions at energies normal for tetragonal Cu^{2+}.[18] The interaction is strong enough to correlate the electron spins and produce a singlet ground state,[27] but the orbitals are otherwise nearly independent. In this situation there are four possible $O_2^{2-} \rightarrow Cu^{2+}$ charge-transfer transitions, labeled A_1, A_2, S_1, and S_2 in Figure 6. Differences in energy and intensity between A_1 and A_2, and between S_1 and S_2, can arise from Cu^{2+} inequivalency and from interaction of the transition dipoles.[18] There is evidence from circular dichroism spectroscopy[28] and from the Raman excitation profile of the O-O stretching mode[3] that the broad visible absorption of oxyHc contains at least two transitions, one at ~570 and the other at ~490 nm (1.75 and 2.04 μm^{-1}). Freedman et al.[3] assigned these to transitions from the two different O_2^{2-} π^* orbitals, but the suggested assignment of Solomon and co-workers[18] corresponds to S_1 and S_2. Their assignment of the 345-nm (2.9 μm^{-1}) band corresponds to A_1 and/or A_2; the two components may be too close in energy to be resolved, or one may be much weaker than the other, or hidden by other absorptions. The intensity disparity between the near-UV and visible absorption bands is consistent with better overlap of π_A^* than π_S^* with the Cu^{2+} orbitals. This assignment places the stabilization of π_A^* relative to π_S^* at about 1.0 μm^{-1}, over twice the value observed for binuclear Co(III) peroxo complexes.[29]

Cu–Cu Interaction and the Electronic Raman Band. The antiferromagnetic coupling between the Cu^{2+} ions is determined by the orbital interactions with the bridging ligand orbitals, as discussed by Hoffmann and co-workers.[27] While the O_2^{2-} orbitals must play a role, the dominant interaction may be with the other postulated bridging ligand,[1] X, in view of the diamagnetism of metHc from which oxyHc can be generated by addition of O_2^{2-}.[18] A plausible candidate for X is the oxygen atom of a tyrosine side chain. This would be consistent with data on ethoxyformylated Hc and spectrophotometric tyrosine titration,[30] and with the observation in low-temperature absorption spectra, of both met- and oxyHc, of a band near 400 nm, assignable to phenolate $\rightarrow Cu^{2+}$ charge transfer.[18] Phenolate-bridged binuclear Cu^{2+} complexes do not seem to have been characterized, but the structurally analogous pyridine *N*-oxide bridged complexes are known to show strong antiferromagnetic interaction, with $-2J \simeq 1000$ cm^{-1}, because of the rather large Cu-O-Cu angle.[31] For oxyHc, $-2J$ has been estimated to be >625 cm^{-1}, from the lack of detectable paramagnetism at room temperature.[5]

The energy gap between the ground singlet state and the triplet state of the coupled Cu^{2+} ions is expected to be equal to $-2J$.[27] In view of this, the singlet $\rightarrow$ triplet transition is an attractive assignment for the 1075-cm^{-1} electronic Raman band which we observe in oxyHc. This band is resonant with the 345-nm transition, and hence is associated with the Cu^{2+} ions. The energy is too low to correspond to a d-d transition on a single tetragonal Cu^{2+} ion. The difficulty with a singlet $\rightarrow$ triplet assignment is that such a transition is spin forbidden, and has never previously been established for binuclear Cu^{2+} complexes, either via IR or Raman spectroscopy. Similar transitions have recently been assigned to features of the RR spectra of iron-sulfur proteins,[32,33] but we have been unable to reproduce these features.[34] The Raman transition polarizability is expected to be proportional to the square of the resonant (345 nm) transition dipole moment times the spin-orbit coupling between the singlet and triplet states. Although the spin-orbit constant[35] for Cu^{2+} (~830 cm^{-1}) is modest, the energy gap between the coupled states, 1075 cm^{-1}, is relatively small, and the matrix element might be of the same order of magnitude as vibrational Franck-Condon products. Combined with the large resonant dipole strength, this could account for the observation of a singlet-triplet transition in our RR spectra.

Raman Enhancements and Vibrational Assignments. The Raman enhancement of the O-O stretching mode via the visible transitions can be understood in terms of the O-O bond shortening attendant on the removal of an electron from the upper π^* orbital. The mode is enhanced by an approximately equal factor in the near-UV transition; since the Raman enhancement scales as the square of the transition dipole moment, the Franck-Condon product for the O-O stretch must be about 400 times smaller in the near-UV excited state, the absorptivity at 345 nm being 20 times larger than that at 570 nm. This disparity may stem from the large energy difference between the two π^* O_2^{2-} orbitals. The lower energy π^* orbital, which is associated with the 345-nm band, is less antibonding than the higher energy orbital, and the O-O bond is less affected by the loss of a π^* electron.

The large enhancements observed for the low-frequency Cu-ligand modes in resonance with the 345-nm band must reflect the antibonding character of the terminal Cu orbital. This orbital, being the only half-filled Cu^{2+} orbital, is oriented toward the set of ligands exerting the strongest ligand field, and it is not surprising that copper-imidazole modes should be strongly involved in the transition. Only two copper-imidazole stretching modes, at 226 and 267 cm^{-1}, are definitely assignable from D_2O frequency shifts, but the shoulders at 287, 315, and 337 cm^{-1} are also candidates, since small D_2O shifts would not have been detectable. Alternatively, one or two of them could arise from stretching modes of the postulated bridging ligand X (the frequency separation between in- and out-of-phase Cu-X-Cu modes depends on the deviation of the Cu-X-Cu angle from 90°[36]). The simplest assignment would be ν_{Cu-X} at 337 and 315 cm^{-1}, and ν_{Cu-Im} at 287, 267, and 226 cm^{-1}.

These frequencies are in the range observed for tetragonal copper-imidazole complexes,[3] as shown in Table III. The Raman spectra of $Cu(ImH)_4^{2+}$ salts show Raman bands at ~250 cm^{-1}, assignable to the breathing mode, and IR bands at ~290 cm^{-1}, assignable to the E_u asymmetric stretch. Interestingly, the tetrakis complexes with 1- or 2-methylimidazole show a 25-cm^{-1} increase in the breathing mode, although a decrease would have been expected on the basis of increased mass. A possible explanation is a steric distortion of the tetragonal structure induced by the methyl groups, with an ex-

pansion of the N-Cu-N angles from 90° and a concomitant shortening of the Cu-N bonds. Such a distortion would be expected to lengthen the axial Cu-Cl bonds; consistent with this the Cu-Cl Raman mode decreases from 208 cm^{-1} in $Cu(ImH)_4Cl_2$ to 200 cm^{-1} in $Cu(2\text{-}MeImH)_4Cl_2$ and to 191 cm^{-1} in $Cu(1\text{-}MeIm)_4Cl_2$.

The intense 267-cm^{-1} oxyHc band is also somewhat above the 250-cm^{-1} breathing frequency of $Cu(ImH)_4^{2+}$, while the 226-cm^{-1} band is appreciably lower. We interpret the lower frequency as reflecting a contribution of an axial imidazole ligand in a square-pyramidal complex, according to the model of the hemocyanin binding site proposed in the preceding paper.[1] The 267-cm^{-1} mode is assignable to the in-phase stretch of the basal imidazole ligands; an appreciable mixing between the two modes is expected, and is required to explain the 226-cm^{-1} intensity, since the apical imidazole ligand would not interact appreciably with the antibonding $d_{x^2-y^2}$ orbital on Cu^{2+}. The 287-cm^{-1} mode is assignable to the out-of-phase stretch of the basal imidazole ligands. The asymmetric disposition of the imidazole ligands in the model is also consistent with the appreciable $^{63}Cu/^{65}Cu$ isotope shift seen for all three modes; the rigid imidazole rings have a higher effective mass than the bridging groups, O_2^{2-} and X, and appreciable copper motion is expected in all three modes. On the other hand, in view of the possibility that the two Cu^{2+} coordination groups are not equivalent, it cannot be excluded that the different Raman bands may be associated with Cu-Im modes on different Cu atoms, although some overlap would be likely. The different intensity patterns observed for mollusc and arthropod hemocyanins might be explained on this basis. The highest intensity is observed at 267 cm^{-1} for molluscs but at 287 cm^{-1} for arthropods, and this might arise from the superposition of slightly different modes in the two proteins.

The lack of enhancement for any mode assignable to $Cu\text{-}O_2$ stretching is puzzling. Appreciable overlap of the O_2^{2-} π_A^* orbital with the Cu^{2+} $d_{x^2-y^2}$ orbital is implied by the large transition moment of the 345-nm band. Yet the failure to observe a resonance-enhanced $Cu\text{-}O_2$ mode suggests very little change of the $Cu\text{-}O_2$ bond length in the charge-transfer excited state. This inference seems to require that the orbital interaction responsible for the charge-transfer transition plays an insignificant role in the $Cu\text{-}O_2$ bond energy. This may be a consequence of a high degree of ionicity in the bond, consistent with the low value of the O-O stretching frequency, which is characteristic of ionic peroxides.[3]

Conclusions

1. The RR spectra can be understood on the basis of the assignment of the visible and near-UV absorption bands of oxyHc to charge-transfer transitions from the two different O_2^{2-} π^* orbitals. The much lower Franck-Condon product for the near-UV transitions implied by the enhancement factors of the O-O stretch is consistent with the lower energy π^* orbital being less antibonding with respect to the O-O bond. However, the failure to detect a $Cu\text{-}O_2$ stretching mode, despite the substantial overlap between Cu^{2+} and O_2^{2-} orbitals implied by the high 345-nm absorptivity, is puzzling.

2. H_2O/D_2O frequency shifts confirm the assignment of the 226- and 267-cm^{-1} bands to Cu-Im modes. The $^{63}Cu/^{65}Cu$ isotope shifts for these bands as well as the one at 287 cm^{-1} imply an asymmetric disposition of the imidazole ligands, consistent with a square-pyramidal model, with an apical imidazole. The frequencies themselves also support the model.

3. The broad RR band at 1075 cm^{-1} is plausibly assigned to the singlet → triplet transition of the coupled Cu^{2+} ions. A sizable coupling between the two states, together with the large enhancement available with the 345-nm resonance, may explain the observation of a spin-forbidden Raman transition.

Acknowledgments. We thank Professors H. S. Mason and E. I. Solomon for the gift of hemocyanin samples. We are also indebted to Professor Solomon and Drs. J. Hare and P. Stein for helpful discussions concerning the electronic assignments. This work was supported by National Institutes of Health Grant GM 13498.

References and Notes

(1) J. Brown, L. Powers, B. Kincaid, J. A. Larrabee, and T. G. Spiro, *J. Am. Chem. Soc.*, preceding paper in this issue.
(2) J. S. Loehr, T. B. Freedman, and T. M. Loehr, *Biochem. Biophys. Res. Commun.*, **56**, 510 (1974).
(3) T. B. Freedman, J. S. Loehr, and T. M. Loehr, *J. Am. Chem. Soc.*, **98**, 2809 (1976).
(4) T. J. Thamman, J. S. Loehr, and T. M. Loehr, *J. Am. Chem. Soc.*, **99**, 4187 (1977).
(5) E. I. Solomon, D. M. Dooley, R-H. Wang, H. B. Gray, M. Cerdonio, F. Mogno, and G. L. Romani, *J. Am. Chem. Soc.*, **98**, 1029 (1976).
(6) D. M. Kurtz, Jr., D. F. Shriver, and I. M. Klotz, *J. Am. Chem. Soc.*, **98**, 5033 (1976).
(7) J. A. Larrabee, T. G. Spiro, N. S. Ferris, W. H. Woodruff, W. A. Maltese, and M. S. Kerr, *J. Am. Chem. Soc.*, **99**, 1979 (1977).
(8) T. C. Strekas, D. H. Adams, A. Packer, and T. G. Spiro, *Appl. Spectrosc.*, **28**, 324 (1974).
(9) H. A. DePhillips, Jr., K. W. Nickerson, and K. E. Van Holde, *J. Mol. Biol.*, **50**, 471 (1970).
(10) A. Ghiretti-Magaldi and G. Nardi in "Protides of the Biological Fluids", Vol. 11, H. Peeters, Ed., Elsevier, New York, 1964, pp 507–950.
(11) G. D. Parker, "Mellors Modern Inorganic Chemistry", Longmans, Green and Co., New York, 1961, pp 653–654.
(12) (a) W. J. Ellbeck, F. Holmes, and A. E. Underhill, *J. Chem. Soc. A*, 757 (1967). (b) W. J. Ellbeck, F. Holmes, C. E. Taylor, and A. E. Underhill, *J. Chem. Soc. A*, 128 (1968).
(13) H. Woodruff and T. G. Spiro, *Appl. Spectrosc.*, **28**, 74–75 (1974).
(14) D. F. Shriver and J. B. R. Dunn, *Appl. Spectrosc.*, **28**, 319–323 (1974).
(15) B. C. Cornilsen and K. Nakamoto, *J. Inorg. Nucl. Chem.*, **36**, 2467–2471 (1974).
(16) J. L. Markley, *Acc. Chem. Res.*, **8**, 70–80 (1975).
(17) S. Salama and T. G. Spiro, *J. Am. Chem. Soc.*, **100**, 1105–1111 (1978).
(18) R. S. Himmelwright, N. C. Eickman, and E. I. Solomon, *Proc. Natl. Acad. Sci. U.S.A.*, **76**, 2094 (1979).
(19) J. B. R. Dunn, D. F. Shriver, and I. M. Klotz, *Proc. Natl. Acad. Sci. U.S.A.* **70**, 2582–2584 (1973).
(20) T. G. Spiro and B. P. Gaber, *Annu. Rev. Biochem.*, **46**, 553 (1977).
(21) R. C. Lord and N. J. Yu, *J. Mol. Biol.*, **50**, 509 (1970).
(22) J. M. Isangaris, J. W. Cheng, and R. B. Martin, *J. Am. Chem. Soc.*, **91**, 726–731 (1969).
(23) J. Tang and A. C. Albrecht, "Raman Spectroscopy", Vol. 2, H. A. Szymanski, Ed., Plenum, New York, 1970, pp 33–67.
(24) T. G. Spiro and P. Stein, *Annu. Rev. Phys. Chem.*, **28**, 501–521 (1977).
(25) A. Warshel, *Annu. Rev. Biophys. Bioeng.*, **6**, 273–300 (1977).
(26) H. J. Schugar, E. I. Solomon, W. L. Cleveland, and L. Goodman, *J. Am. Chem. Soc.*, 6442–6450 (1975).
(27) P. J. Hay, J. C. Thibeault, and R. Hoffmann, *J. Am. Chem. Soc.*, **97**, 4884 (1975).
(28) K. E. Van Holde, *Biochemistry*, **6**, 93–99 (1967).
(29) V. M. Miskowski, J. L. Robbins, I. M. Treitel, and H. B. Gray, *Inorg. Chem.*, **4**, 2318 (1975).
(30) Y. Engelborgh and R. Lontie, *Eur. J. Biochem.*, 335–341 (1973).
(31) R. W. Jothan, S. F. A. Kettle, and J. A. Marks, *J. Chem. Soc., Dalton Trans.*, 1133 (1972).
(32) H. Blum, F. Adar, J. C. Salerno, and J. S. Leigh, Jr., *Biochem. Biophys. Res. Commun.*, **77**, 650–657 (1977).
(33) F. Adar, H. Blum, J. S. Leigh, Jr., F. Ohnishi, J. Salerno, and J. Kimura, *FEBS Lett.*, **84**, 214–216 (1977).
(34) J. R. Hare and T. G. Spiro, unpublished observations.
(35) B. N. Figgis, "Introduction to Ligand Fields", Wiley, New York, 1966, p 60.
(36) R. M. Wing and K. P. Callahan, *Inorg. Chem.*, **8**, 871 (1969).